Benchmarking of vertically integrated models for the study of the impact of caprock morphology on CO2 migration

Ahmadinia, M., Shariatipour, S. M., Andersen, O. & Sadri, M.

Original citation & hyperlink:
Ahmadinia, M, Shariatipour, SM, Andersen, O & Sadri, M 2019, 'Benchmarking of vertically integrated models for the study of the impact of caprock morphology on CO2 migration' International Journal of Greenhouse Gas Control, vol. 90, no. November 2019, 102802.
https://dx.doi.org/10.1016/j.ijggc.2019.102802

DOI 10.1016/j.ijggc.2019.102802
ISSN 1750-5836

Publisher: Elsevier

Benchmarking of vertically integrated models for the study of the impact of caprock morphology on CO_2 migration

Masoud Ahmadinia[1,*], Seyed M. Shariatipour[1], Odd Andersen[2], Mahdi Sadri[1]

[1] Centre for Fluid and Complex Systems, Coventry University, UK
[2] Digital, Mathematics and Cybernetics Department, Oslo, Norway
* Correspondence: Ahmadinm@uni.coventry.ac.uk

Abstract

Saline aquifers constitute the most abundant geological storage option for Carbon Capture and Storage (CCS) projects. When injected in the aquifer, due to its lower density in comparison to the in-situ brine, the free phase CO_2 tends to migrate upwards. This vertical migration is generally tens of metres depending on the reservoir thickness, despite the plume migration distance in the horizontal direction which could be over hundreds of kilometres (depending on the time horizon, reservoir characteristics, trapping mechanisms involved, etc.). In many situations, the plume ends up as a separate region below a sealing barrier. This large aspect ratio between the plume migration in the horizontal and vertical directions would potentially validate the use of vertical equilibrium (VE) models in CO_2 storage studies. In other words, when phase segregation occurs rapidly compared to the time scale studied, vertical equilibrium can be assumed, allowing for the use of specially adapted models. In the VE model, the equilibrium between brine and CO_2 is pre-assumed at all times. Under this assumption, the injected CO_2 plume flow in 3D can be approximated in terms of its thickness in order to obtain a 2D simulation model, which consequently decreases the computational costs. The time by which phase segregation occurs depends on the aquifer thickness, aquifer permeability, fluid properties, etc. However, the CO_2 and in-situ brine are separated considerably fast and form two separate layers, in comparison to the time period for lateral migration.

The CO2lab module of the Matlab Reservoir Simulation Toolbox (MRST) used in this work, is a set of open source simulation and workflow tools to study the long-term, large-scale storage of CO_2. We employed the VE tool in MRST-CO2lab (MVE) to study the effect of caprock morphology on the CO_2 migration. The results have been compared with a number of simulators including ECLIPSE-black-oil (E100), ECLIPSE-compositional (E300) and ECLIPSE-VE (EVE) models and the differences between the approaches are analysed and discussed in detail. In particular, we focused on the impact of caprock morphology and aquifer top-surface slope on the CO_2 structural and dissolution trapping mechanisms and plume migration. The results indicated a good agreement for the ultimate plume shapes in all the models. However, the amount of dissolved CO_2 in the brine was different.

1. Introduction

Numerical simulators are important tools for studying problems related to the safe storage of CO_2 in saline aquifers. They have become essential when investigating safety, feasibility and economic concerns related to a CCS project. Therefore, it is important that we have confidence in the results provided by numerical simulators, and understand how sensitive their responses are with respect to storage site parameters.

One of the key sensitivity issues when modelling CO_2 storage is caprock geometry, both at the large and smaller scale (Ahmadinia, Shariatipour, & Sadri, 2019; Onoja& Shariatipour, 2018). The caprock geometry of the sedimentary rocks is usually deformed with geological time which results in structures such as tilted beds and folds. Sinusoidal structures which are formed through both deformation and deposition processes are common in sedimentary rocks. They are observed in different scales from which folds and bedforms are the main types (Han& Kim, 2018). Folds which are the results of non-isostatic pressure (stress) and are the largest type of sinusoidal features have three broad classes, namely anticlines, synclines and monoclines. The first two types which are generally the results of regional folding are of our interest in this study. Bedforms can be found in a wide range of environments such as eolian and fluvial. These sine-wave shaped morphological features are usually formed at the interface between the bed and fluid (Mountney, Posamentier, & Walker, 2006).

As discussed, occurrences of dipping strata and sine-wave structures are widespread in geological settings. In the literature (Jones et al., 2009; Pringle et al., 2010), rugosity refers to the topography variation which is smaller than the typical seismic resolution (around 10 m) and is recognisable using LiDAR scanning of outcrops. The current study assumes that such heterogeneous features (rugosity and dipping strata) are preserved in the targeted storage site, could impact the CO_2 plume storage and trapping process.

The model data representing the formation characteristics will always be uncertain in the 3D simulation of the CO_2 storage. Regardless of the predominant driving force in the model, the presence of heterogeneity may considerably alter the plume migration path. Most of the aquifers, in reality, have complex geology, such as Sleipner in the North Sea which has a complex layered structure. The detailed modelling of the aquifer is not always available due to the limited number of exploration wells and a dearth of seismic data. While the plume migration path in the long-term is governed by the caprock morphology, oversimplified top surfaces are sometimes considered in simulation studies (Shariatipour, Seyed M., Pickup, & Mackay, 2016).

Current approaches are unable to fully resolve the problems involved in the relevant physics, upscaling, and numerical modelling in the practical simulation of CO_2 in geological formations. Therefore, the problem needs to be simplified to be computationally feasible. A benchmark study was performed (Nordbotten, J. M. et al., 2012) using three distinct approaches including reduced physics, upscaling and non-converged discretisation to simplify the problem. The CO_2 storage in a simplified aquifer was simulated using different simulation approaches to answer relevant storage questions. The results for the various simulation method and assumption were divergent which shows that even with highly idealised problems, the numerical simulation tools are not providing convincing results.

For this study, we employed the CO2lab module in MRST (Bao et al., 2017) and the results have then been compared with three numerical solutions provided by ECLIPSE software, namely E300, E100 and EVE. It is worth to mention that E300 is a compositional simulator, and thus differs significantly from the three others which are all based on the black-oil formulation. The Matlab Reservoir Simulation Toolkit (MRST) has been developed by the Computational Geoscience Group within the Department of Mathematics and Cybernetics at the division of SINTEF Digital in Norway. The CO2lab module is based on the vertical equilibrium assumption which facilitates the modelling of large-scale CO_2 migration. Vertical equilibrium method supports modelling of most relevant physical effects involved in long-term migration, and its applicability on realistic models has been the topic of multiple past studies (Ahmadinia& Shariatipour, 2019; Bandilla, Karl& Celia, 2019; Court et al., 2012; Gasda, Nordbotten, & Celia, 2009; Nilsen, Lie, & Andersen, 2016a). After being injected, the supercritical CO_2 may potentially migrate several hundreds of kilometres in the horizontal direction,

with very limited vertical movement (typically tens of meters), (Shariatipour, Seyed M. et al., 2016). For long-term storage of CO_2, plume migration is controlled by gravity and capillary forces (Bjørnarå et al., 2014). Since the gravity segregation is often a fairly short timescale process (due to the difference between the fluid densities), the plume will eventually form a thin layer beneath the caprock after the injection has ended (Ahmadinia et al.). Thus, the vertical fluid segregation is prompt compared with the up-dip migration and we can assume that the fluids are fully segregated and are in vertical equilibrium.

It is possible to formulate the VE model in a black oil simulation framework as it has the same structure for multiphase flows as traditional equations. The VE model in the MRST (MVE) is based on fully implicit solvers and is adaptable to industry standards (Nilsen, Lie, & Andersen, 2016b). As mentioned above, the VE assumption is valid for the long-term storage of the CO_2 where the timescale is larger than the vertical segregation time. It should be noted that the VE model avoids errors caused by vertical discretisation, but is built on the assumption of vertical equilibrium, and will, therefore, introduce modelling errors of its own if this assumption is not justified. When using the VE method, the layer heterogeneity in permeability is ignored which is a source of error and may invalidate the single-layer VE approach if there are strong vertical variation in permeability. However, some recent studies (Møyner& Nilsen, 2017; Møyner, Andersen, & Nilsen, 2018) have applied VE in a multilayer setting with strong permeability contrast, combined with full 3D discretisation locally where needed. The errors introduced by VE assumption are in many cases smaller than the errors induced by low lateral resolution grids to make the 3D simulations computationally feasible (Nilsen et al., 2016a). Moreover, benchmark studies (Class et al., 2009; Nordbotten, J. M. et al., 2012) show that 3D numerical simulations are sometimes challenging and the important enquiries concerning the CO_2 sequestration cannot be forecasted convincingly, even in a highly idealised problem.

In a VE simulation model, the problem dimension is reduced to 2D. The significant reduction in the number of unknowns of the 2D system compared to the 3D system significantly reduces the computational cost of the problem. Therefore, it allows the modeller to e.g. increase lateral grid resolution beyond what would be otherwise practical for 3D simulations. Using the upscaled 2D variables from the VE formulations, it is possible to reconstruct the 3D solution through analytical calculations. VE assumption can be considered a special case of the more general Dupuit assumption (Bear, 2013), which states in an unconfined flat aquifer with hydrostatic groundwater, the water discharge is proportional to the thickness of the saturated aquifer. Many researchers (Coats et al., 1967; Coats, Dempsey, & Henderson, 1971; Martin, 1958; Martin, 1968) used similar models several decades ago in the petroleum industry. The performance of a number of 3D numerical methods has been investigated (Class et al., 2009) on specific problems related to the CO_2 storage in geological models. The results showed a reasonable degree of agreements. The major sources of error were believed to be due to gridding, wrong inputs and different interpretations of the problem (such as boundary conditions).

There are some benchmark studies comparing the performance simulations tools in CO_2 storage problems. Early comparison of full 3D simulation and VE calculations on a real model was done on the Utsira formation in (Nilsen et al., 2011). In that paper, a simplified model that did not include capillary pressure and dissolution was considered. The results showed that the VE model was significantly faster than the 3D simulation for the case studied. Moreover, when segregation is achieved, the solutions provided by the VE models were more accurate than their 3D counterparts. The spatial distribution of reservoir permeability was modified to find a match the observed and calculated plume extension data for the Sleipner model. The authors (Cowton et al., 2018) developed a vertically integrated fluid flow simulator and their results were nearly identical to those of E100. A

number of (10 in total) mathematical and numerical models were applied (Class et al., 2009) to three different benchmark studies including: Leakage of injected CO_2 into overlying formations through a leaky well, enhanced gas recovery (EGR) by injection of CO_2 and CO_2 plume spreading and dissolution and storage mechanisms in a large-scale heterogeneous reservoir. According to their study, realistic heterogeneities and uncertainties, due to different ways of incorporating heterogeneity within the applied spatial discretisation, have a noticeable impact on the results. A simplified CO_2 storage study was designed (Nordbotten, J. M. et al., 2012) to understand the extent of variability in model predictions resulted by applying different modelling approaches to the same problem. Six research groups participated using the 3D simulator (4 groups), MVE and analytical approaches. Despite considering a relatively simple, idealised problem the resulted model predictions varied significantly. The source of errors was mainly due to a difference in physical processes (such as dissolution and capillary pressure), numerical modelling approaches, upscaling and interpretation of problem definition.

To our knowledge, this is one of the first benchmark studies on the impact of caprock morphology on CO_2 storage migration using a number of modelling approaches (E100, E300, EVE and MVE). Especially, we have investigated the impact of small-scale, sinusoidal undulations in the caprock (which we refer to as 'rugosity') on CO_2 plume migration and dissolution trapping. For this purpose, we constructed 15 sets of 3D geological models with a wide range of rugosity and slopes in Matlab; and systemically analysed the performance of 4 simulation tools in a CO_2 storage study. The objective is to show the benefits of using VE approach for CO_2 migration and dissolution in a geological model while focusing on a realistic caprock morphology.

2. Mathematical formulation

In this section, the governing equations for the flow dynamics in the VE and 3D models are compared. Equation 1 describes the mass conservation in the 3D simulations on the fine scale,

$$\frac{\partial(\varphi\rho_\alpha s_\alpha)}{\partial t} + \nabla.\rho_\alpha u_\alpha = \rho_\alpha q_\alpha \qquad \text{Equation 1}$$

where,

α: fluid phase (w or g),

φ: porosity,

ρ_α: fluid density,

s_α: phase saturation,

q_α: phase volumetric flux,

u_α: is the fluid velocity, given by Darcy's equation

$$u_\alpha = -k\lambda_\alpha(\nabla p_\alpha - \rho_\alpha g) \qquad \text{Equation 2}$$

where,

k: rock absolute permeability,

λ_α: fluid mobility,

$\lambda_\alpha = \lambda_\alpha\,(s_w) = \frac{k_{r\alpha}(s_w)}{\mu_\alpha}$, $k_{r\alpha}$ and μ_α denote for relative permeability and fluid viscosity respectively

p_α: fluid pressure,

g: gravitational acceleration,

Replacing the parameters in Equation 1 with their vertically integrated counterparts, it is possible to derive the governing equation for the vertical equilibrium approach. For simplicity, a sharp interface between the fluids is assumed. A detailed derivation can be found in (Bandilla, Karl W., Celia, & Leister, 2014; Møll Nilsen et al., 2011; Nilsen et al., 2016b). Here we present the final mass conversation relation in the VE model. Plume thickness below the caprock is used as a variable to present the equation in fractional form (Nilsen et al., 2017).

$$\Phi\frac{\partial h}{\partial t}+\nabla f(h)\left(U_t-k\left(\varrho_w-\varrho_g\right)\Lambda_g(h)\Lambda_w(H-h)g\nabla(z_t+h)\right)=Q_g \qquad \text{Equation 3}$$

where,

h: plume thickness,

H= aquifer thickness,

Φ: porosity,

ϱ_α: phase density,

z_t: top surface depth,

U_t: total volume flux which is given by Darcy's equation,

$$U_t=-k\Lambda_t(h)(\nabla p_i-[\rho_w-\left(\rho_w-\rho_g\right)f_g(h)]g\nabla(z_t+h)) \qquad \text{Equation 4}$$

where,

p_i: pressure at the interface of gas and water,

f_g: fractional flow function for gas phase which is given by,

$$f_g=\Lambda_g(h)/[\Lambda_w(H-h)+\Lambda_g(h)] \qquad \text{Equation 5}$$

It is important to note that upscaled mobility (Λ_t in Equation 4) is different from the fine scale (λ_α in Equation 2) and is defined as (Nordbotten, Jan Martin& Celia, 2011):

$$\Lambda_\alpha\equiv\int_{\xi_B}^{\xi_I}\lambda_{\alpha,||}k_{||}dz\,\boldsymbol{K}^{-1} \qquad \text{Equation 6}$$

where,

ξ_B= elevation of the bottom of the formation (surface),

ξ_I= elevation at which two fluids are separated (surface),

$\boldsymbol{K}^{-1}$= integrated permeability,

The upscaled parameters in VE formulation are obtained by integrating the fine-scale ones across the thickness of the aquifer with respect to the z. Therefore despite λ_α which depends on three spatial parameters 'x', 'y' and 'z', Λ_t depends on 'x' and 'y' only (In addition to time). Several models are available for the reconstruction of fine-scale saturation and mobility based on the upscaled saturation, out of which we employed the sharp interface. The method is valid when the capillary pressure effect is negligible in the 3D model. More details can be found in (Andersen, Gasda, & Nilsen, 2015). Both ECLIPSE and MRST have implemented their equation using finite-volume discretisation that is fully implicit in time.

2.1.Dissolution in E300, E100, EVE and MVE

CO_2 dissolves into the brine and saturates at values of a few percents per volume. The CO_2 dissolution algorithm provided by CO2STORE keyword in E300 allows the carbon dioxide to dissolve in the aqueous phase. The fugacity function for aqueous CO_2 is constructed to match solubility data, based on which the equilibrium between aqueous CO_2 and brine is defined. E300 in the current study uses

Peng-Robison equation of state to compute the fluid properties at their corresponding temperature and pressure (Schlumberger, 2017). The CO_2 solubility in water is a function of temperature, pressure and salinity which is calculated from the Chang et al. correlation (Chang, Coats, & Nolen, 1996).
The fluid properties in E100 are provided from two dimensional (Brine and dissolved CO_2) tabular data which are a function of pressure and are interpolated and extrapolated if required, at a constant slope. The tables for E100 can be derived from the E300 fluid inputs, using the PVTi program in ECLIPSE to make sure the input properties are identical. Therefore, E100 and E300 input properties are identical with a high degree of accuracy, and the only difference is in their formulation method which is black oil and compositional in E100 and E300, respectively.
Vertical Equilibrium in Eclipse (EVE) is an option in E100. Using this option, despite the saturation data (Which are used to calculate relative permeability and capillary pressures) other rocks and fluid properties and also simulation approach in EVE are identical to the E100. In E100 dispersed (Rock curve, in which the fluids are assumed to be evenly distributed over the grid block) saturation function is specified, while EVE enables us to specify either dispersed or segregated (VE assumption, where fluids are in hydrostatic equilibrium) saturation functions, or a weighted average of the two. Therefore, dissolution in EVE is handled the same way as it is in E100, i.e. using the PVT tables.
While using MVE, CO_2 and brine are assumed to be separated by a sharp interface which leads to an upscaled relative permeability function that is linear (Nilsen et al., 2016a). Viscosity and compressibility are interpolated from the sampled table (identical to the one used in other simulations) within the desired temperature and pressure range. CO_2 and brine have completely segregated into different regions, with CO_2 on the top and brine on the bottom. In such a fully segregated system, dissolution occurs only in the interface region. Since CO_2 saturated brine at the interface is denser than the ambient brine, convective mixing may be triggered that significantly enhances the dissolution by transporting saturated brine away from the two-phase region and downwards into the vertical column. This process happens naturally in sufficiently resolved 3D simulators, but in MVE dissolution is mainly governed by the constant upscaled "rate" value and a maximum dissolution parameter. The "rate" is constant and unique for this particular study and depends on both rock and fluid properties. In order to set an accurate value for this "rate", before starting the main benchmark study, we performed some simulation using E300 and calculated the gas flow rate for an individual block. Using this flow rate, the average downward migration speed of CO_2 during the post-injection period is calculated, then it is possible to estimate the suitable up-scaled rate value for the MVE. After making sure that the "rate" is a good representative of the dissolution happening in the 3D simulations, we performed the benchmark study.

3. Numerical simulations

3.1. Model setup

The purpose of this study is to investigate the outcomes of different simulation approaches applied to the models with various rugosity and aquifer top-surface slope. We compare long-term plume development, the amount of dissolved CO_2, and computational requirements. For this purpose, a homogeneous closed boundary aquifer was defined, to which we add rugosity and slope depending on the specific test case. The horizontal permeability is 50 mD which is in the range of In Salah storage site. CO_2 is injected through one centred injector for ten years with a rate of 0.5 Mt/year, which is comparable to 20% of the emissions of a 500 MW coal-fired power plant (Orr, 2009). The injection is then followed by 1000 years of post-injection migration.

Details of aquifer parameters are available in Table 1.

Table 1. Aquifer parameters

Parameter		**Value**
Number of cells (NX×NY×NZ)		201×201×9
Reservoir size (km) (LX×LY×LZ)		40×40×0.1
Cell size (m)	DX×DY	199×199
	DZ	5 (layers 1-4) 10 (layers 5-7) 25 (layers 8-9)
Rock compressibility (1/bars)		4.35E-5
Water density at 1500 m depth (kg/m^3)		1049
CO_2 density at 1500 m depth (kg/m^3)		468
Residual water saturation (S_{rw})		0.27
Residual CO_2 saturation (S_{rc})		0.20
Horizontal Permeability k_h (mD)		50
Vertical to horizontal to Permeability (k_v/k_h)		0.1
Porosity		0.2
Pressure at the 1500 m depth (bar)		147
Simulation period (years)		1010
Number of time steps		200 (100*0.1 years + 100*10 years)
Water viscosity at 150 bar (Centipoise)		0.444
CO_2 viscosity at 150 bar (Centipoise)		0.033
Reservoir Temperature		80^{o}C

The relative permeability curves are shown in Figure 1.

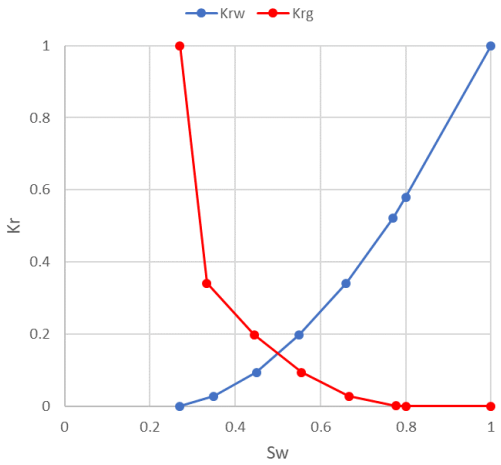

Figure 1. Relative permeability curves (Smith et al., 2012)

Four parameters including the aquifer top-surface slope and amplitude of the rugosity in x and y directions were chosen for our sensitivity analysis. The contact boundary between the caprock and reservoir is described by the following formula:

$$z(x,y) = \mathrm{A}[\sin(\omega_b x) + \sin(\omega_b y)] - R_x \sin(\omega_c x) - R_y \sin(\omega_c y) + x\tan(S_x) + y\tan(S_y) \quad \text{Equation 7}$$

where $\omega = \frac{2\pi}{\lambda}$ is the angular frequency of the sine wave function and z, x and y are the z, x and y-directional coordinate of the caprock surface, respectively.

The terms A, ω_b and ω_c are constant in Equation 7 at the values of 40 (m), 25 (rad/m) and 150 (rad/m) respectively while R_x, R_y, S_x and S_y are unique for each case. The first two terms (with "A" as a multiplier) represent the main structural traps. The next two negative terms represent rugosity which has a higher frequency than the main structural traps ($\omega_c > \omega_b$). The next two tangential terms represent the model tilt angles. The amplitude of rugosity, and model dip angles in x and y directions are represented by R_x, R_y, S_x and S_x which are the sensitivity analysis parameters in this study.

The base case model is flat (not tilted, $S_x = S_y = 0$), without rugosity ($R_x = R_y = 0$) and the caprock is presented local domes only using the first two terms in Equation 7 (Figure 2). The amplitude of the dome is 40 m, having $R_{x,y} = 20$ add a sinusoidal structure with an average amplitude of 20 m to the dome.

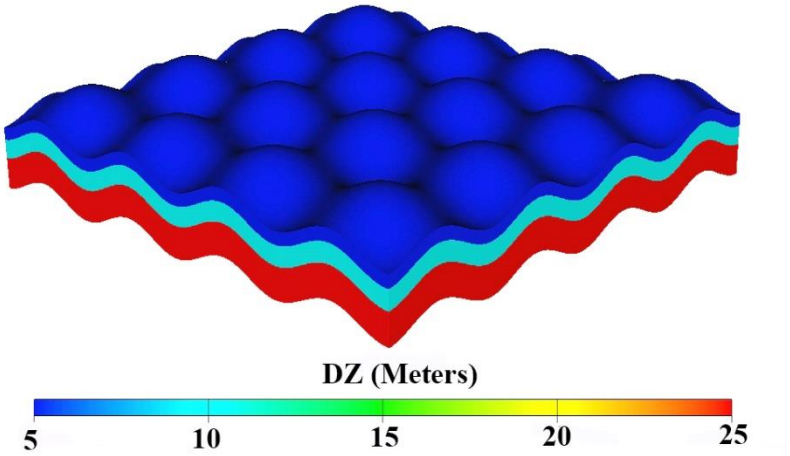

Figure 2. Thickness of Base case (Not to scale)

In order to analyse quantitatively how dipping and small-scale structures affect the CO_2 storage process, a function was written in Matlab to construct the geological models using different rugosity and slope in x and y-direction. The models (Table 2) were then automatically imported into MVE, E100, E300 and EVE simulators separately and their corresponding results for CO_2 dissolution and computational time were analysed in Matlab (124 simulations in total). The list of simulation cases is available in Table 2.

Table 2. List of simulation cases

Case #	R_x (m)	R_y (m)	S_x (°)	S_y (°)	Case #	R_x (m)	R_y (m)	S_x (°)	S_y (°)
BASE	0	0	0	0	**8**	20	0	0	0
1	0	0	0	5	**9**	20	0	0	5
2	0	0	5	0	**10**	20	0	5	0
3	0	0	5	5	**11**	20	0	5	5
4	0	20	0	0	**12**	20	20	0	0
5	0	20	0	5	**13**	20	20	0	5
6	0	20	5	0	**14**	20	20	5	0
7	0	20	5	5	**15**	20	20	5	5

3.2. Justification of constant temperature assumption

The shallowest part of the domain corresponds to 1.5 km depth and a constant temperature of 80°C is considered in all the models. The impact of temperature becomes more significant in the tilted models. The highest tilt angle in this study is 5° which results in the following condition (Figure 3):

- CO_2 will be injected at the depth of 3.25 km, which is feasible in CO_2 storage studies such as Rousse site in France (4 km) and Weyburn in Canada (3.8km) (Espinoza& Santamarina, 2017).
- The temperature at the top of the model (1.5 km depth) is 80°C.
- The temperature at the injection point (3.25 km depth, middle) is 115°C.
- The temperature at the upmost of the plume (2.55 km depth) is 101°C.

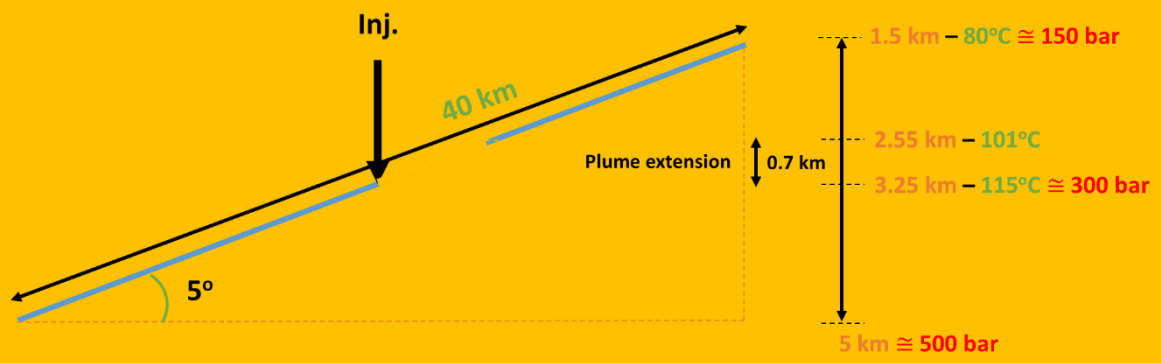

Figure 3. Reservoir condition in 5° inclined models.

If we compare the tilted models (injection point at 3.25 km, 115 °C) with flat models (injection point at 1.5 km, 80 °C), considering a constant temperature, we ignore 35°C (115 °C-80 °C=35 °C) change in temperature (which is also equivalent to the distance from injection point to the top of the model in tilted models). In other words, in this study, the temperature is at a constant value of 80 °C while the real temperature at the injection point in the models with 5° tilt would be 115 °C. According to the CO_2 solubility data in water (Kohl& Nielsen, 1997), a change in temperature from 80°C to 115°C at 300 bars (pressure at the injection point in tilted models, Figure 3), results in 0.2% error in CO_2 solubility. Based on theoretical data, at high temperature and pressure conditions (such as this study), CO_2 solubility becomes a weak function of temperature which makes the constant temperature assumption feasible. We performed three sets of experiments using E300 to support this argument. The surface temperature varies between 0-30°C (Bachu, 2003). We chose 15°C as the surface temperature and considered three sets of geothermal gradient including:

- Exp1: A geothermal gradient of 43°C/km until the depth of 1.5km, followed by 20°C/km from 1.5km downward which is the same condition as shown in Figure 3. A related point to consider is that we have real cases with abnormal geothermal gradients within certain depth such as Soultz-sous-Forêts (Gérard et al., 2006) in which at the depth of 1000m geothermal gradient is 100°C/km and decreases to 50 °C/km at 2000m.
- Exp2: A constant geothermal gradient of 20°C/km.
- Exp3: A constant geothermal gradient of 43.3°C/km.

Details of the geothermal gradients in all the experiments are available in Figure 4.

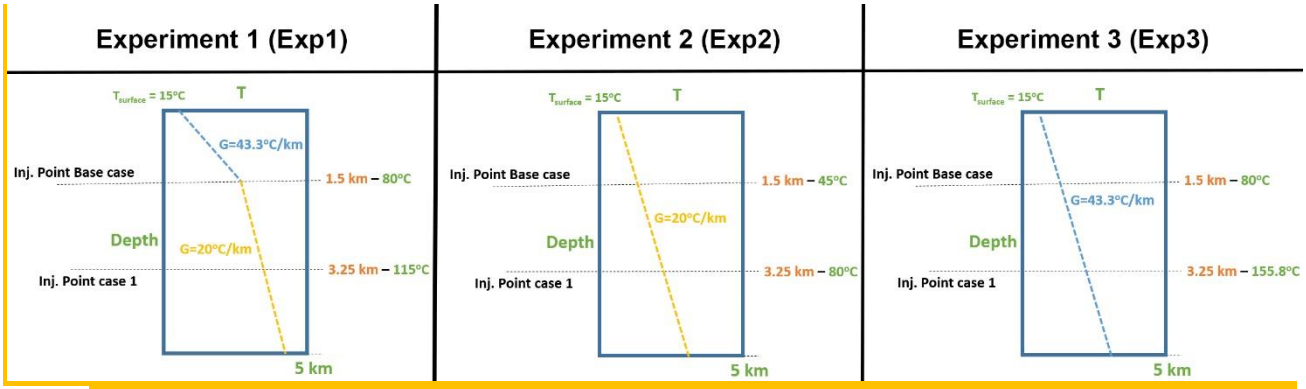

Figure 4. Temperature versus depth data in all the experiments.

We performed simulation using Base Case (0,0,0,0) and Case 1 (0,0,0,5) in E300 considering the temperature versus depth data presented in Figure 4. The averaged absolute errors between the results from these experiments and the ones from the paper are reported in Table 3. In this study, we considered a constant temperature of 80°C which means in both tilted and flat cases the CO_2 is injected at this temperature. The corresponding injection temperature for Base Case in Exp1 and Exp3 and Case 1 in Exp2 is also 80°C (Figure 4) which explains the minimum averaged absolute errors in these scenarios.

Table 3. The averaged absolute error between the results from the experiments and the ones from the paper for Base Case and Case 1.

	The averaged absolute error		
	Exp1	**Exp2**	**Exp3**
Base Case (0,0,0,0)	0.99%	5.29%	2.01%
Case 1 (0,0,0,5)	4.51%	1.92%	5.36%

These results confirm our observation from the CO_2 solubility data in water (Kohl& Nielsen, 1997) and show that regardless of the temperature gradient (Exp1, Exp2 or Exp3), at our operation condition (above 150 bars and at 80°C), the impact of temperature on the overall dissolution are fairly negligible.

3.3.Simulation results

There is good agreement between the final plume distribution results from the ECLIPSE (E100, E300 and EVE) and MRST (MVE) models. The CO_2 plume saturation in the top cells of the base case was compared with four cases (4, 5, 11 and 12) at the end of the simulation in Figure 5. It is clear that the plume migrates farther in tilted models (Case 4 vs 5) while having rugosity on the top surface limits its migration extent (Bases case vs 12).

The upscaled (VE) saturation is not the true fine scale (3D) saturation but the one by assuming hydrostatic fluid pressure distribution in the vertical direction. The upscaled saturation is the fraction of CO_2 in a total vertical column, which is basically the variable 'h' divided by aquifer thickness (when disregarding residual saturation). To present the vertical equilibrium results more effectively, 3D CO_2 saturations are reconstructed from the VE solution for the mobile and residual CO_2 interfaces and then projected onto a 3D image. For this purpose, based on the value of calculated CO_2 thickness, saturation values are allocated to the corresponding cell in the 3D grid. For more information see (Nilsen, Lie et al. 2016).

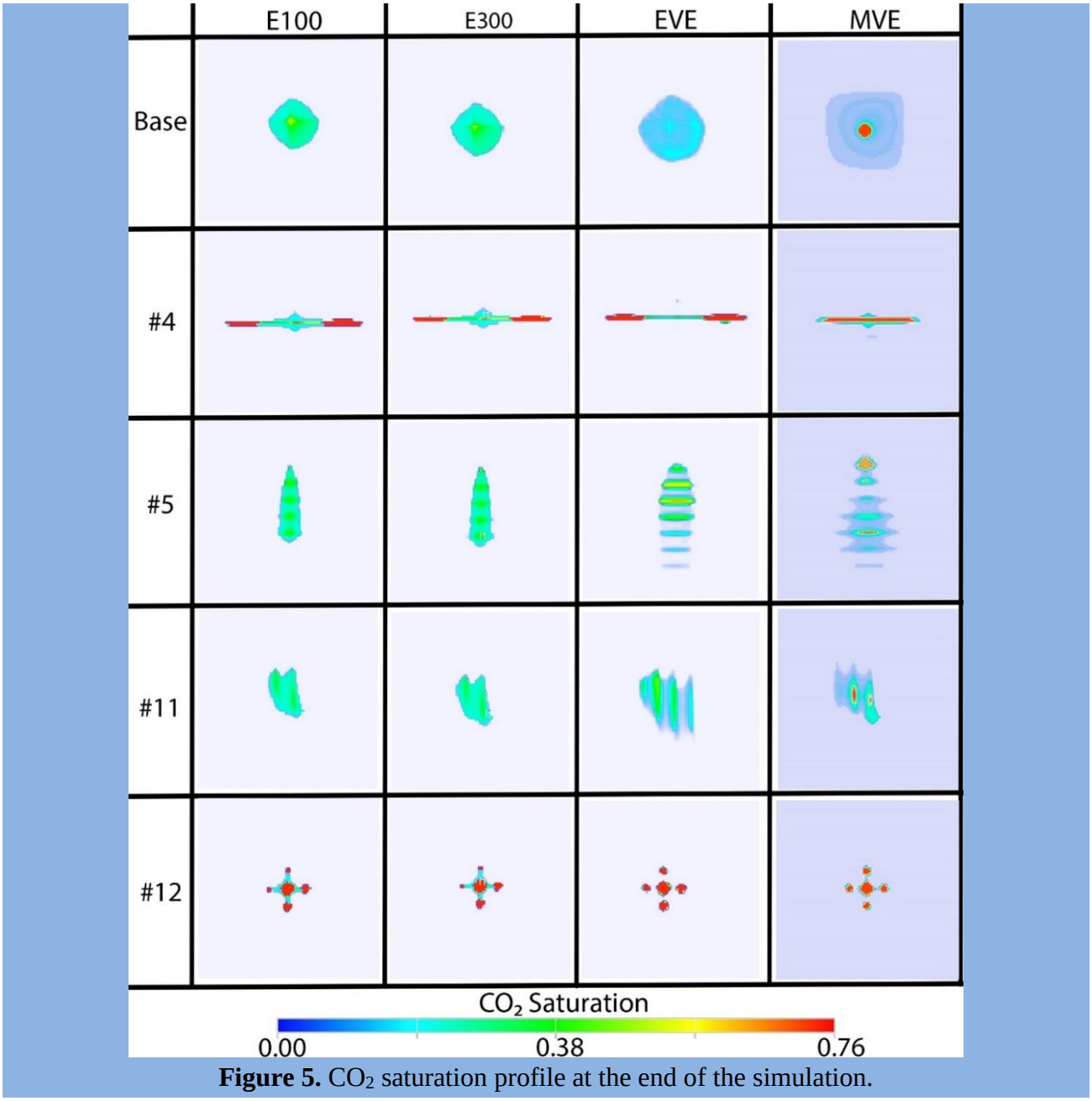

Figure 5. CO_2 saturation profile at the end of the simulation.

The extent of the plume is seen to be higher in the VE model (EVE and MVE) which could be partially due to the earlier segregation, and partially due to the numerical diffusion caused by limited vertical resolution in the 3D model. The other reason is that since the vertical permeability is 5 mD, the plume spreads much longer before reaching to the top which eventually part of the plume becomes trapped residually while moving upward in 3D simulations (E100 and E300). However, in the VE model, the plume's upwards migration is instantaneous. Figure 6 clearly validates this statement. The top and side (middle layer) views of the plume distribution are illustrated for the E300 and EVE model. The plume extent at each end is shown with an arrow. It is clear that a noticeable portion of the CO_2 becomes residually trapped in E300 model in bottom layers which consequently results in lower migration distance/speed.

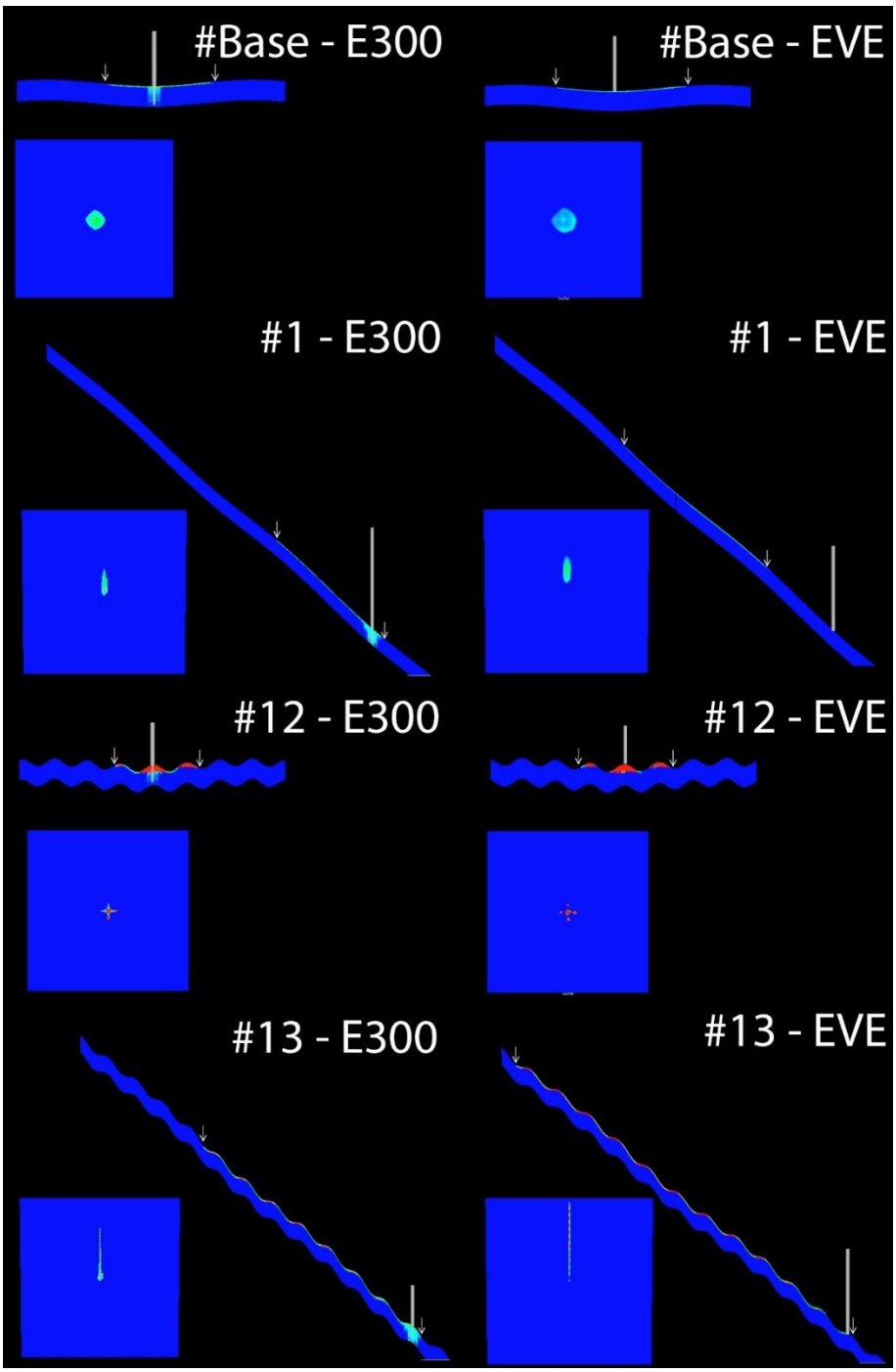

Figure 6. The side and top views of plume distribution in E300 and EVE models.

The percentage of CO_2 dissolution for all the cases is presented in Figure 7. Here we have investigated the amount of dissolved CO_2 at the end of injection, at mid-way and the end of the simulation. Based on the current simulation parameters, using formula (19) from (Andersen& Nilsen, 2018) segregation time can be shown to be on the order of 20 years for this scenario. The results indicate that there is a discrepancy in the early stages (10 years, which is less than segregation time), which is likely caused by the VE assumption not being approximately valid at this point. The dissolution is seen to be higher in the VE models (EVE and MVE) than 3D (E100 and E300). As mentioned above, when using the VE model, the plume migrates to the top of the aquifer instantly, which consequently results in increased contact with fresh brine, higher migration distances and as a result higher dissolution. This statement is consistent with the two different trends we observed for the VE and 3D models as well. For instance, while the dissolution is higher in the Base Case (R_x=0, R_y=0, S_x=0, S_y=0 or 0,0,0,0) than Cases 1 (0,0,0,5) in the 3D models, the trend is opposite for the VE models. This is due to the

fact that by increasing the aquifer slope, the cone-shaped CO_2 plume around the well area extends further upslope, thereby increasing in volume and leading to more residual trapping of CO_2 (Figure 6). In other words, the plume migration distance becomes smaller in the 3D than VE models which result in less contact with in-situ brine in farther distances and therefore lower dissolution. In order to confirm this argument, for Bases Case (0,0,0,0) and Cases 1 (0,0,0,5) we increased the horizontal and vertical permeability to 500mD and 50mD respectively. The results show an increase in the amount of dissolution by increasing the tilt angle in both E100 and E300. The corresponding amount of dissolved CO_2 in brine for both simulators for the Bases Case (0,0,0,0) and Cases 1 (0,0,0,5) became 39.1% and 41.6% while with lower permeability they were 31.1% and 27.2% respectively. In the flat cases, the injected CO_2 moves upwards vertically with limited lateral migration at bottom layers (compared to the tilted models), eventually resulting in lower residual trapping and therefore higher dissolution. Figure 6 also shows that the residual trapping in the Base Case and Case 12 (20,20,0,0) is lower than their equivalent tilted models which are Cases 1 (0,0,0,5) and 13 (20,20,0,5) respectively. A similar conclusion was reported in previous studies (Shariatipour, S. M., Pickup, & Mackay, 2016), where the dissolution was seen to decrease by increasing the tilt in the models with low vertical permeability. Moreover, to assure that the resulted dissolution trend is not due to the error introduced by low vertical resolutions, the Base Case (0,0,0,0) and Case 1 (0,0,0,5) were refined to 90 cells in the vertical direction (i.e. 1m vertical resolution). The results remained relatively unchanged and as it was observed before, the dissolution in the tiled model (Case 1) became lower than the flat one (Base case).

Another reason for having different behaviours in the amount of dissolution in 3D and vertical equilibrium models is possibly due to the differences in fluid properties and saturation data. (See section 2.1).

The results for the E100 and E300 are aligned throughout the simulation. While both VE approaches show similar overall trends, the MVE shows a higher dissolution which might be due to differences in how dissolution is actually modelled in the EVE and MVE models as described in the previous paragraph. The minimum dissolution occurs in the flat model with rugosity in both the x and y directions (#12), which is due to the fact that the plume becomes immobilised in small structural traps (Figure 6). In this case, even in 3D models, increasing the slope results in a higher dissolution, so as a consequence Cases 13 (20,20,0,5) have a higher dissolution than Case 12 (20,20,0,0), which was not the case for Cases 1 (0,0,0,5) versus the Base case (0,0,0,0). As it is clear in figure 6, the plume extent in Case 13 (20,20,0,5) is significantly higher than Case 12 (20,20,0,0) for both E300 and EVE models.

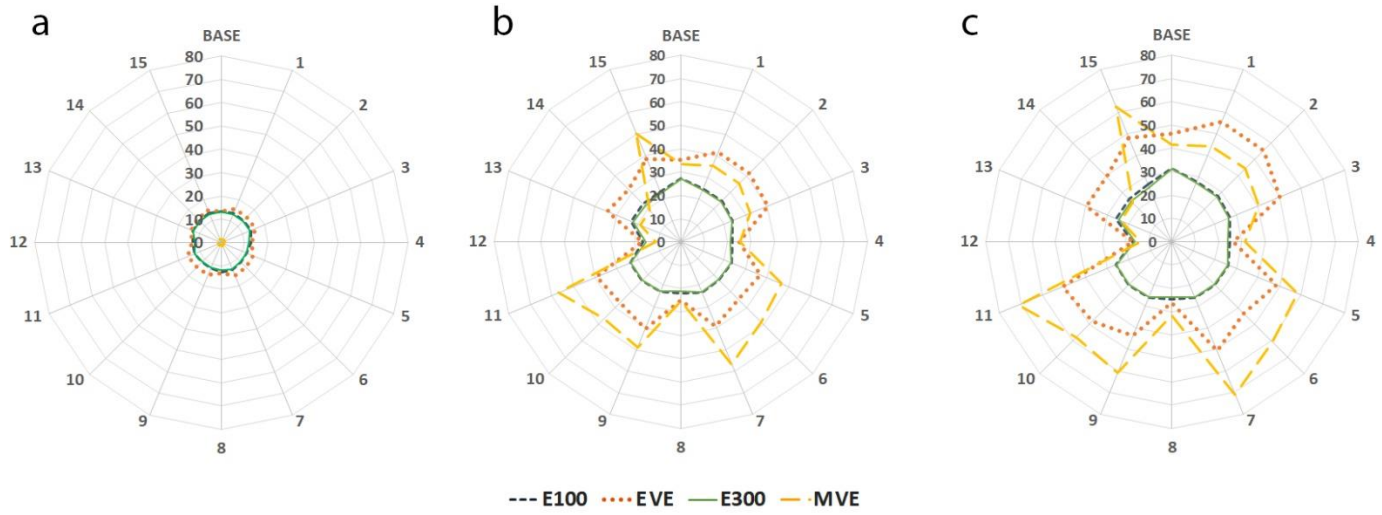

Figure 7. CO_2 dissolution in the aquifer (percentage of total injected CO_2), for all the cases after 10 (a), 500 (b) and 1010 (c) years.

Figure 8 shows the simulation time for all the models. The computational time is evaluated using the same hardware for all the simulations. As expected, both VE models have significantly lower computational cost than the 3D simulators. Top surface rugosity and tilt do not appear to play any major role for the computational time.

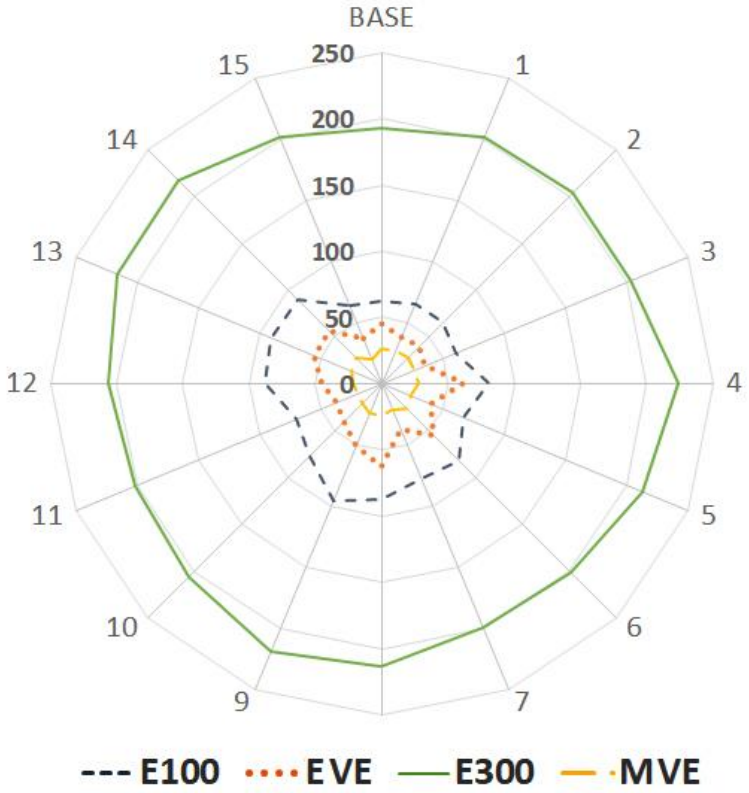

Figure 8. Simulation time for all the cases (minutes)

4. Conclusion and remarks

In this study, we compared the performance of four simulation models including EVE, E100, E300 and MVE. The simulations were performed on a homogenous model with a fairly low permeability of 50 mD and 5 mD in the horizontal and vertical directions, respectively. The impact of the reservoir

slope on dissolution in 3D simulators was found to be different from what we expected in high permeability aquifers. As reported in previous studies, we observed that increasing the tilt angle resulted in farther migration and greater contact with the brine, which consequently increases the dissolution (Pruess& Nordbotten, 2011; Wang et al., 2016). However, in this study, the trend in 3D simulators was seen to be the opposite, and the dissolution was seen to decrease by increasing the tilt angle, which is thought to be due to residual trapping of the plume in lower layers due to limited vertical permeability. Therefore the match between the results from VE and 3D simulators which were observed in previous studies might not be the case in tight reservoirs. The results showed a good agreement between the plume shapes in all the models. Concerning the computation costs, MVE significantly outperformed the E100, E300 and EVE models.

5. Acknowledgement

The authors would like to thank the Centre for Fluid and Complex Systems at Coventry University for providing financial support for this project. The authors also wish to thank Schlumberger for the use of the ECLIPSE software and SINTEF for the use of MRST. Special thanks also to Dr Phil Costen for reviewing the paper and sharing his constructive comments with us.

6. References

Ahmadinia, M., & Shariatipour, S. (2019). Investigating the Impact of Caprock Morphology on the CO_2 Plume Migration and Trapping Mechanism Using Mrst-CO2lab and Eclipse. *14th Greenhouse Gas Control Technologies Conference Melbourne 21-26 October 2018 (GHGT-14)*. Available at SSRN: https://ssrn.com/abstract=3366371.

Ahmadinia, M., Shariatipour, S. M., Andersen, O., & Sadri, M.A history matching approach to estimate caprock morphology parameters for CO_2 storage in saline aquifers. *SPE Europec featured at 81st EAGE Conference and Exhibition*. Society of Petroleum Engineers, 2019.

Ahmadinia, M., Shariatipour, S. M., & Sadri, M. (2019). A Comprehensive Sensitivity Analysis on CO_2 Plume Migration and Trapping under Tilted Sinusoidal Structures. *81st EAGE Conference & Exhibition. 3 - 6 June 2019*. London.

Andersen, O., Gasda, S. E., & Nilsen, H. M. (2015). Vertically Averaged Equations with Variable Density for CO_2 Flow in Porous Media. *Transport in Porous Media, 107*, 95-127.

Andersen, O., & Nilsen, H. M. (2018). Investigating simplified modeling choices for numerical simulation of CO_2 storage with thermal effects. *International Journal of Greenhouse Gas Control, 72*, 49-64.

Bachu, S. (2003). Screening and ranking of sedimentary basins for sequestration of CO_2 in geological media in response to climate change. *Environmental Geology, 44*, 277-289.

Bandilla, K. W., Celia, M. A., & Leister, E. (2014). Impact of Model Complexity on CO_2 plume modeling at Sleipner. *Energy Procedia, 63*, 3405-3415.

Bandilla, K., & Celia, M. (2019). Numerical Modeling of Fluid Flow During Geologic Carbon Storage. In Anonymous *Science of Carbon Storage in Deep Saline Formations* (pp. 137-157). Elsevier.

Bao, K., Lie, K., MÃ¸yner, O., & Liu, M. (2017). Fully implicit simulation of polymer flooding with MRST. *Computational Geosciences, 21*, 1219-1244.

Bear, J. (2013). *Dynamics of fluids in porous media.* Courier Corporation.

Bjørnarå, T. I., Mathias, S. A., Nordbotten, J. M., Park, J., & Bohloli, B. (2014). Capturing the coupled hydro-mechanical processes occurring during CO_2 injection–example from In Salah.

Chang, Y., Coats, B. K., & Nolen, J. S. (1996). A compositional model for CO_2 floods including CO_2 solubility in water.

Class, H., Ebigbo, A., Helmig, R., Dahle, H. K., Nordbotten, J. M., Celia, M. A., Audigane, P., Darcis, M., Ennis-King, J., Fan, Y., Flemisch, B., Gasda, S. E., Jin, M., Krug, S., Labregere, D., Naderi Beni, A., Pawar, R. J., Sbai, A., Thomas, S. G., Trenty, L., & Wei, L. (2009). A benchmark study on problems related to CO_2 storage in geologic formations. *Computational Geosciences, 13*, 409.

Coats, K., Dempsey, J., & Henderson, J. (1971). The use of vertical equilibrium in two-dimensional simulation of three-dimensional reservoir performance. *Society of Petroleum Engineers Journal, 11*, 63-71.

Coats, K., Nielsen, R., Terhune, M. H., & Weber, A. (1967). Simulation of three-dimensional, two-phase flow in oil and gas reservoirs. *Society of Petroleum Engineers Journal, 7*, 377-388.

Court, B., Bandilla, K. W., Celia, M. A., Janzen, A., Dobossy, M., & Nordbotten, J. M. (2012). Applicability of vertical-equilibrium and sharp-interface assumptions in CO_2 sequestration modeling. *International Journal of Greenhouse Gas Control, 10*, 134-147.

Cowton, L., Neufeld, J., White, N., Bickle, M., Williams, G., White, J., & Chadwick, R. (2018). Benchmarking of vertically-integrated CO_2 flow simulations at the Sleipner Field, North Sea. *Earth and Planetary Science Letters, 491*, 121-133.

Espinoza, D. N., & Santamarina, J. C. (2017). CO_2 breakthrough—Caprock sealing efficiency and integrity for carbon geological storage. *International Journal of Greenhouse Gas Control, 66*, 218-229.

Gasda, S. E., Nordbotten, J. M., & Celia, M. A. (2009). Vertical equilibrium with sub-scale analytical methods for geological CO_2 sequestration. *Computational Geosciences, 13*, 469.

Gérard, A., Genter, A., Kohl, T., Lutz, P., Rose, P., & Rummel, F. (2006). The deep EGS (Enhanced Geothermal System) project at Soultz-sous-Forêts (Alsace, France). *Geothermics, 35*, 473-483.

Han, W. S., & Kim, K. (2018). Evaluation of CO_2 plume migration and storage under dip and sinusoidal structures in geologic formation. *Journal of Petroleum Science and Engineering, 169*, 760-771.

Jones, R. R., McCaffrey, K. J. W., Clegg, P., Wilson, R. W., Holliman, N. S., Holdsworth, R. E., Imber, J., & Waggott, S. (2009). Integration of regional to outcrop digital data: 3D visualisation of multi-scale geological models. *Computers & Geosciences, 35*, 4-18.

Kohl, A. L., & Nielsen, R. (1997). *Gas purification.* Elsevier.

Martin, J. C. (1968). Partial integration of equations of multiphase flow. *Society of Petroleum Engineers Journal, 8*, 370-380.

Martin, J. C. (1958). Some mathematical aspects of two phase flow with application to flooding and gravity segregation. *Prod.Monthly, 22*, 22-35.

Møll Nilsen, H., Herrera, P. A., Ashraf, M., Ligaarden, I., Iding, M., Hermanrud, C., Lie, K., Nordbotten, J. M., Dahle, H. K., & Keilegavlen, E. (2011). Field-case simulation of CO_2 -plume migration using vertical-equilibrium models. *Energy Procedia, 4*, 3801-3808.

Mountney, N. P., Posamentier, H., & Walker, R. (2006). Eolian facies models. *SPECIAL PUBLICATION-SEPM, 84*, 19.

Møyner, O., Andersen, A., & Nilsen, H. M. (2018). Multi-model hybrid compositional simulator with application to segregated flow.

Møyner, O., & Nilsen, H. M. (2017). Multiresolution Coupled Vertical Equilibrium Model for Fast Flexible Simulation of CO_2 Storage. *Computational Geosciences 23.1 (2019): 1-20.*

Nilsen, H. M., Herrera, P., Ashraf, S. M., Ligaard, I. S., Iding, M., Hermanrud, C., Lie, K., Nordbotten, J. M., Dahle, H. K., & Keilegavlen, E. (2011). Field-case simulation of CO_2-plume migration using vertical-equilibrium models.

Nilsen, H. M., Krogstad, S., Andersen, O., Allen, R., & Lie, K. (2017). Using sensitivities and vertical-equilibrium models for parameter estimation of CO_2 injection models with application to Sleipner data. *Energy Procedia, 114*, 3476-3495.

Nilsen, H. M., Lie, K., & Andersen, O. (2016a). Fully-implicit simulation of vertical-equilibrium models with hysteresis and capillary fringe. *Computational Geosciences, 20*, 49-67.

Nilsen, H. M., Lie, K., & Andersen, O. (2016b). Robust simulation of sharp-interface models for fast estimation of CO 2 trapping capacity in large-scale aquifer systems. *Computational Geosciences, 20*, 93-113.

Nordbotten, J. M., & Celia, M. A. (2011). *Geological storage of CO_2: modeling approaches for large-scale simulation.* John Wiley & Sons.

Nordbotten, J. M., Flemisch, B., Gasda, S. E., Nilsen, H. M., Fan, Y., Pickup, G. E., Wiese, B., Celia, M. A., Dahle, H. K., Eigestad, G. T., & Pruess, K. (2012). Uncertainties in practical simulation of CO2 storage. *International Journal of Greenhouse Gas Control, 9*, 234-242.

Onoja, M. U., & Shariatipour, S. M. (2018). The impact of gradational contact at the reservoir-seal interface on geological CO_2 storage capacity and security. *International Journal of Greenhouse Gas Control, 72*, 1-13.

Orr, F. M. (2009). Onshore Geologic Storage of CO_2. *Science, 325*, 1656.

Pringle, J. K., Brunt, R. L., Hodgson, D. M., & Flint, S. S. (2010). Capturing stratigraphic and sedimentological complexity from submarine channel complex outcrops to digital 3D models, Karoo Basin, South Africa. *Petroleum Geoscience, 16*, 307-330.

563 Pruess, K., & Nordbotten, J. M. (2011). Numerical Simulation Studies of the Long-term Evolution of
564 a CO_2 Plume in a Saline Aquifer with a Sloping Caprock. *Transport in Porous Media, 90*, 135-151.

565 Schlumberger (2017). ECLIPSE Technical Description.

566 Shariatipour, S. M., Pickup, G. E., & Mackay, E. J. (2016). Simulations of CO_2 storage in aquifer
567 models with top surface morphology and transition zones. *International Journal of Greenhouse Gas*
568 *Control, 54, Part 1*, 117-128.

569 Shariatipour, S. M., Pickup, G. E., & Mackay, E. J. (2016). Investigation of CO_2 storage in a saline
570 formation with an angular unconformity at the caprock interface. *Petroleum Geoscience, 22*, 203-
571 210.

572 Smith, M., Campbell, D., Mackay, E., & Polson, D. (2012). *CO_2 aquifer storage site evaluation and*
573 *monitoring: Understanding the challenges of CO_2 storage: results of the CASSEM project.* Scottish
574 Carbon Capture and Storage.

575 Wang, F., Jing, J., Xu, T., Yang, Y., & Jin, G. (2016). Impacts of stratum dip angle on CO_2 geological
576 storage amount and security. *Greenhouse Gases: Science and Technology, 6*, 682-694.

577